Crystallization and Structure Formation of Block Copolymers Containing a Rubbery Amorphous Component

Tomoo Shiomi,* Hiroki Takeshita, Hiroshi Kawaguchi, Masaru Nagai, Katsuhiko Takenaka, and Masamitsu Miya

Department of Materials Science and Technology, Nagaoka University of Technology, Nagaoka, Niigata 940-2188, Japan

Received January 7, 2002; Revised Manuscript Received July 19, 2002

ABSTRACT: Changes of higher-order structure of poly(ethylene glycol)−poly(butadiene) (PEG−PBd) di- and triblock copolymers in isothermal crystallization from microphase-separated melts were studied using time-resolved synchrotron small-angle X-ray scattering (SR−SAXS) techniques. Lamellar microphase structure of PEG−PBd with weight fractions $f_{PEG} = 0.57$ and 0.51 was destroyed on crystallization and changed to a lamellar structure distinct from that in the melt. A diblock copolymer with $f_{PEG} = 0.34$ crystallized, keeping the cylindrical structure preexisting in the melt. On the other hand, a $f_{PEG} = 0.7$ diblock copolymer whose melt structure was cylindrical showed two kinds of structure changes: at low crystallization temperatures T_c the SAXS peak positions changed discontinuously but the structure remained cylindrical, while the structure changed from cylindrical to lamellar at high T_c. Triblock copolymers PBd−PEG−PBd with $f_{PEG} = 0.67$ and 0.42 showed a structure change similar to the $f_{PEG} = 0.57$ and 0.51 diblock copolymers. Behavior of structure changes in the melting process was the reverse of that in the crystallization process for all the samples. Crystallization behavior, in particular crystallization kinetics, was also investigated by DSC and polarized optical microscopy (POM) with a 530 nm retardation plate. Avrami exponents evaluated from DSC results for the block copolymers were almost the same as those for PEG homopolymers even in crystallization from the cylindrical melt, which was quite different from the result in crystallization from a *frozen* microphase-separated melt reported previously. For the $f_{PEG} = 0.34$ diblock and $f_{PEG} = 0.42$ triblock copolymers with a small-sized microdomain in the melt, overall crystallization rates were suppressed and apparent activation energies were high. No spherulite with a clear Maltese cross was observed by POM, but the crystal region was propagated with irregularly distributed blue- and yellow-colored portions for all the block copolymers including the $f_{PEG} = 0.34$ diblock copolymers. This behavior of the propagation and the above result of Avrami exponents for the $f_{PEG} = 0.34$ copolymer suggest that crystallization can traverse from one cylinder domain to another with preservation of the melt structure. From the kinetic results obtained by both DSC and POM, it was suggested that nucleation was easy for the middle block in the triblock copolymers.

1. Introduction

Recently higher-order structure formation in crystallization of semicrystalline block copolymers has been extensively studied[1] using mainly time-resolved small-angle X-ray scattering (SAXS) and wide-angle X-ray scattering (WAXS) techniques. Since block copolymers can have microphase-separation structure in the amorphous state, i.e., a molten state, higher-order structure in the crystalline state may be formed by competition or combination between crystallization and microphase separation. In crystallization below the order−disorder transition temperature (T_{ODT}), it is of main interest whether block copolymers crystallize within a microdomain or not, that is, whether microphase-separation structure in the melt is destroyed by crystallization.

It has been reported that crystallization from a strongly segregated melt is confined to microdomains in the melt. Quiram et al.[2,3] explored that a high molecular-weight ethylene-*b*-(3-methyl-1-butene) (E/MB) block copolymer with a crystallizable component (E) weight fraction (denoted *f*) of 0.27 crystallized within the preexisting cylindrical microdomain. Hamley et al.[4] examined the crystallization of block copolymers containing a hydrogenated 1,4-polybutadiene (PE) from the strongly segregated melt oriented under shear.

In contrast to strongly segregated systems, it has been shown that crystallization from a weakly segregated melt destroys microphase separation structure to form an alternating structure consisting of a crystal lamella and amorphous layer. Nojima et al.[5] investigated a crystallization process for poly(ϵ-caprolactone)-*b*-polybutadiene diblock copolymers (PCL−PBd) through the time-resolved synchrotron−SAXS (SR−SAXS) and observed that a preexisting peak due to the microphase-separation disappeared with development of a new peak related to the long period of crystal lamellae. Ryan et al.[6] also examined the crystallization of a series of block copolymers, whose T_{ODT} was not so high compared with the melting temperature T_m, from cylindrical ($f = 0.25$, 0.75) and lamellar ($f = 0.49$) melts, and found that their melt structures were destroyed by crystallization to be changed to a lamellar structure.

As described above, structural changes on crystallization of block copolymers tend to depend on the segregation strength of the melt. However, even in strongly segregated systems, confined crystallization within the melt microdomain is that from cylindrical domains in most of cases.[2,3] The crystallization confined to lamellar domains is seemed to be limited to the crystallization from *frozen* melts, that is, the block copolymers with a glassy amorphous component such as PE−poly(vinyl cyclohexane)[4] and poly(tetrahydrofuran)−poly(methyl methacrylate) block copolymers.[7]

* To whom correspondence should be addressed.

10.1021/ma0200118 CCC: $22.00
Published on Web 09/13/2002

Furthermore, it has been shown that there is a possibility that the melt structure is maintained even for weakly segregated melts. Rangarajan et al.[8] observed that when the sample was cooled from the melt to a crystallization temperature T_c with similar quench depths below T_{ODT} and T_m, respectively, a sharp Bragg reflection peak due to the melt structure appeared, and during subsequent crystallization, the first-order peak shifted continuously to a lower angle with concurrent appearance and growth of higher-order reflections. Quiram et al.[2] found for a small molecular-weight E/MB block copolymer with $f = 0.26$ that faster cooling confined crystallization to cylinders while slower cooling resulted in complete disruption of the melt structure.

The above observations suggest that the structure change on crystallization from the microphase-separated melt may depend on some other factors in addition to a degree of melt segregation. Since polymers are usually made to crystallize in a condition considerably far from equilibrium, whether the melt structure is maintained or destroyed on crystallization may depend on kinetic aspects such as competition between crystallization and diffusion rates. To examine such effects, in this work, structure changes on crystallization from cylindrical and lamellar melts have been investigated using SR−SAXS for a series of poly(ethylene glycol)-*b*-poly(butadiene) block copolymers (PEG−PBd) with crystallizable PEG weight fractions f ranging 0.3 to 0.7. Although the Flory−Huggins χ parameter in PEG/PBd has not been obtained experimentally as far as we know, PEG−PBd block copolymers are considered to be strongly segregated systems because their T_{ODT} is much higher than PEG's T_m as shown later. Also, the amorphous PBd chains can move flexibly near PEG's T_m because the T_g of PBd is extremely low compared with PEG's T_m.

Kinetics in crystallization from the microphase-separated melts will also be focused on in this paper. Sakurai et al.[9] found very small Avrami exponents in crystallization within a microspace. We[10] also obtained extremely small Avrami exponents and a very high apparent activation energy of crystallization for poly(tetrahydrofuran)-*b*-polystyrene diblock copolymers (PTHF−PS) with $f = 0.49$ and 0.36, and observed no crystallization for $f = 0.27$, where T_m of PTHF is lower than T_g of PS. These results suggest that crystallization from the domain surrounded by a glassy matrix is much restricted. In this paper, crystallization behavior, in particular crystallization kinetics, for PEG−PBd will also be presented to compare with that for the copolymers with such *frozen* melts. Furthermore, crystallization behavior of ABA triblock copolymers in which middle component B is crystalline will be compared with that of diblock copolymers.

2. Experimental Section

2.1. Synthesis and Characterization of Block Copolymers. Block copolymers were prepared by coupling reaction of chain-end brominated PEG with the chain-end anion of living PBd. Poly(ethylene glycol) monomethyl ether supplied kindly by NOF Co. and common PEG purchased from Aldrich Co. were brominated for syntheses of di- and triblock copolymers, respectively. Bromination was carried out using thionyl bromide in dry toluene containing triethylamine. The living PBd precursor was obtained by living anionic polymerization in *n*-heptane for 24 h at 50 °C using *sec*-butyllithium as an initiator. The brominated PEG was reacted with the active chain end of PBd for 3 days at room temperature, and then unreacted PBd was inactivated with ethanol. These polymerization and coupling reactions were carried out successively in a high vacuum system. The polymer products were recovered by precipitation in an excess amount of ethanol. The products thus obtained contained the homopolymers of PBd and PEG and the dimer of PBd as well as PEG−PBd block copolymer. The block copolymer was isolated by the following fractionations: the PEG homopolymer was removed by repeated reprecipitation with a THF/methanol system, then the homopolymer and dimer of PBd were also removed by fractional precipitation carried out by adding diethyl ether to the THF solution, and finally the PEG−PBd block copolymer was isolated by the GPC column fractionation. GPC traces of the final products showed a single peak for all samples.

Table 1. Characteristics of Samples

sample	sample code	$M_n \times 10^{-3}$ PEG[a]	$M_n \times 10^{-3}$ PBd[b]	composition (wt %) PEG	composition (wt %) PBd
PEG	PEG	5.4		100	
PEG−PBd	BE70	5.4	2.3	70	30
	BE57	5.4	4.0	57	43
	BE51	5.4	5.2	51	49
	BE34	5.4	10.5	34	66
PBd−PEG−PBd	BEB67	11.2	2.7 (×2)	67	33
	BEB42	4.6	3.3 (×2)	42	58

[a] Determined by TOF mass. [b] Determined by ^{1}H NMR on the basis of PEG's molecular weight.

Molecular weights of the PBd blocks were determined by ^{1}H NMR on the basis of the molecular weight of the PEG precursor measured by MALDI time-of-flight mass spectroscopy (Voyager DE-RP, PerSeptive Biosystems, Inc.). The distribution of the molecular weight M_w/M_n evaluated by GPC in relative to standard polystyrene was less than 1.09 for all the block copolymers. The amount of 1,2-structure of PBd was evaluated to be 8−10% from the ^{1}H NMR spectra. The molecular weight and the copolymer composition of the samples are shown in Table 1.

2.2. Sample Preparation and Measurements. The block copolymer was dissolved in a good solvent, THF, common to both components to give a 5 wt % solution, and the solution was then dried at room temperature overnight, followed by removing the solvent completely in a vacuum oven at 50 °C for 3 days.

Crystallization and melting processes were observed using time-resolved small-angle X-ray scattering employing synchrotron radiation (SR−SAXS). SR−SAXS measurements were performed using beam line BL-10C at the Photon Factory in the Institute of Materials Structure Science, High Energy Accelerator Research Organization, Tsukuba, Japan. Details of the optics and the instrumentation were described elsewhere.[11] The scattering vector was defined as $q = 4\pi/\lambda \sin(\theta/2)$, where θ is the scattering angle. The sample was annealed in a sample holder kept at 90 °C for 30 min to erase the previous thermal history and to form a stable microphase separation structure. Then, it was moved rapidly into a measurement holder thermostated at a desired crystallization temperature T_c to be crystallized isothermally. The temperature of the measurement holder was controlled by circulating water supplied from a programmable water bath. After the complete crystallization, the sample was heated to 90 °C at ca. 1 °C/min to observe the melting process. The temperature of the sample was monitored during the experiments with a thermister attached to the measurement holder.

DSC measurements were performed with a Parkin Elmer Pyris 1 apparatus. The sample was annealed at 90 °C for 30 min in the DSC apparatus, and then rapidly quenched to a desired T_c. Isothermal crystallization was analyzed by an exothermal peak. After the isothermal crystallization, melting behavior was observed by heating the sample from T_c to 90 °C at 5 °C/min. At a small supercooling degree, because crystallization rates are too slow to detect an exothermal peak clearly, the isothermal crystallization was analyzed by melting peaks at a series of crystallization times.

Crystal growth was observed by polarized optical microscopy using an Olympus BHS-705-P apparatus with a Nikon Coolpix

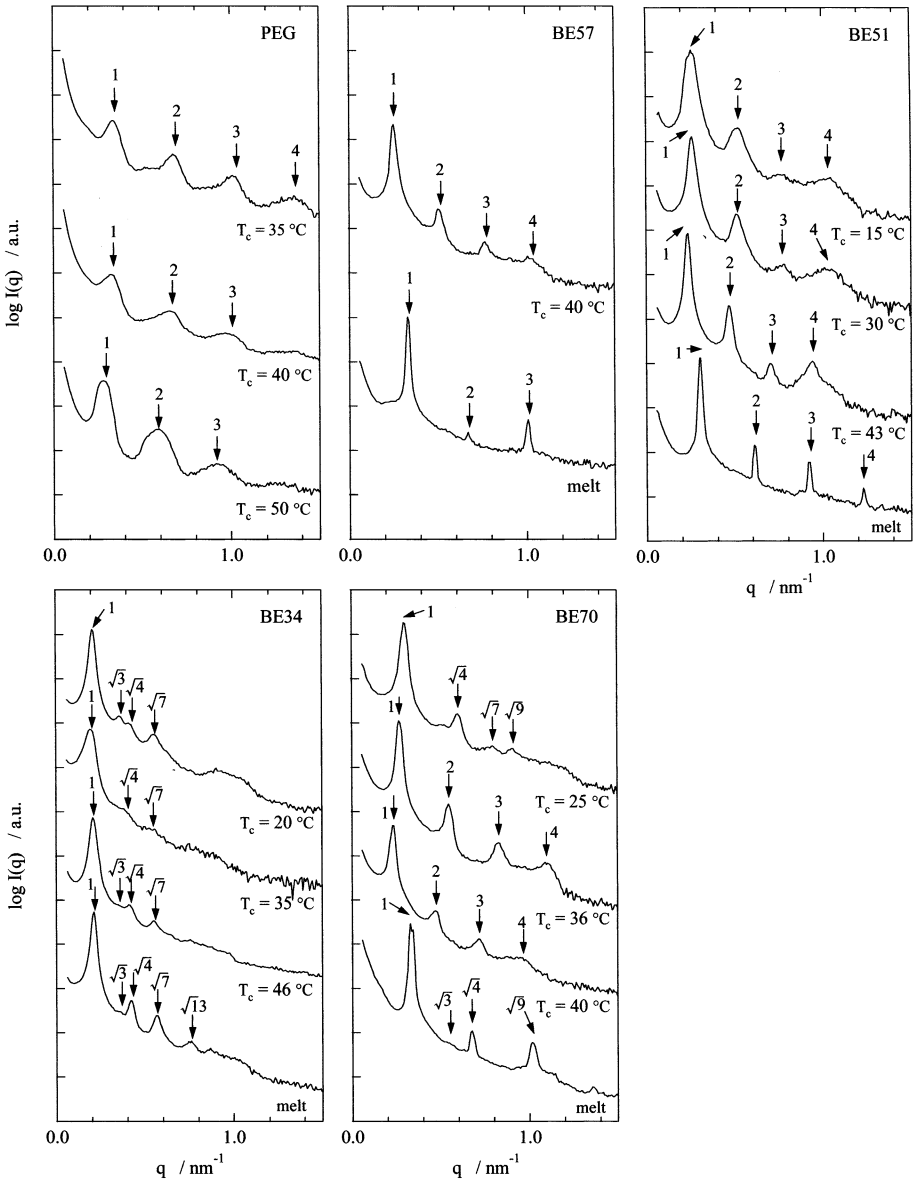

Figure 1. SAXS profiles of PEG homopolymer and PEG−PBd diblock copolymers in the crystalline state at the indicated temperatures and in the molten state.

950 digital camera. The sample was annealed on a hot plate at 90 °C for 30 min and moved rapidly on a measurement hot stage thermocontrolled at T_c, to be crystallized isothermally.

3. Results and Discussion

3.1. Formation of Phase Structure in Crystallization and Melting. (1) Phase Structure in Crystalline and Molten States. Figure 1 shows scattering curves for the PEG homopolymer and diblock copolymers crystallized at the indicated temperatures, together with those in the molten state.

Diffraction peaks of the homopolymer appear at the relative angular position of 1:2:3:4, which indicates lamellar structure consisting of alternatively piled crystalline and amorphous layers as observed usually for crystalline polymers.

For BE51 and BE57 diblock copolymers, the relative positions of the higher-order peaks lie at the ratio of whole numbers in both molten and crystalline states. Namely, the microphase structure in the melt is lamellar as predicted from their copolymer compositions, and the structure in the crystalline state is also lamellar.

For both BE34 and BE70 the first- and higher-order peaks in the melt lie at the relative positions of $1:3^{1/2}:4^{1/2}:7^{1/2}:9^{1/2}:13^{1/2}$, which corresponds to hexagonally packed cylinders. Taking account of their copolymer compositions, the PEG blocks are located in the cylindrical and matrix domains for BE34 and BE70, respectively. The relative peak positions of BE34 in the crystalline state can also be assigned to the cylindrical structure at all crystallization temperatures studied here. On the other hand, BE70 in the crystalline state has cylindrical and lamellar structure at lower crystallization temperatures and at higher temperatures, respectively, than ca. 30 °C. This contrastive behavior between BE34 and BE70 will be discussed later.

As shown in Figure 2, the structure of the triblock copolymers, BEB67 and BEB42, is lamellar in both molten and crystalline states.

(2) Change of Phase Structure in Crystallization and Melting Processes. Figure 3 shows (a) the time development of the scattering curve around the first-order peak and (b) the time dependence of the Bragg spacing in the crystallization process.

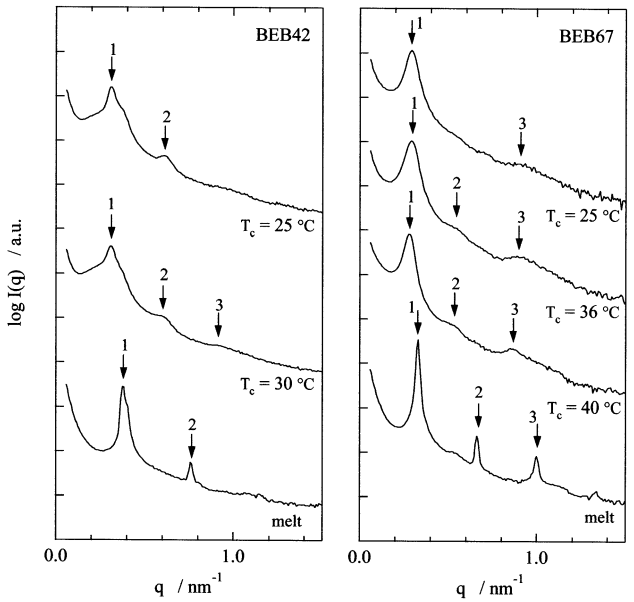

Figure 2. SAXS profiles of PEG−PBd triblock copolymers in the crystalline state at the indicated temperatures and in the molten state.

For PEG homopolymer, as shown in Figure 3-1-a, there is no peak observed just as temperature is jumped from 90 °C to T_c because the homopolymer melt is not microphase-separated, and then a peak related to crystal lamellae appears. The time dependences of the spacing obtained from the peak position at various crystallization temperatures are shown in Figure 3-1-b. The spacing is long in the early stage of crystallization, and then it becomes shorter to be constant. This change of the spacing may come from the fact that all crystal lamellae are not formed simultaneously but gradually with time. The finally reached value of the spacing depends on the crystallization temperature, that is, on the thickness of the crystal lamella.

The peaks of the diblock copolymers in the early stage are due to the microphase separation structure in the melt. In BE51 whose melt structure is lamellar, as seen in the scattering curves of Figure 3-2-a, the intensity of the initial peak decreases as a new peak due to the crystal lamella appears at a smaller q position and develops. This means that the structure is reorganized by crystallization though it changes from lamellar to lamellar. As shown in Figure 3-2-b, as the crystallization temperature is higher, the induction period of crystallization is longer and two kinds of spacing coexist for a longer time.

In BE34 where the morphology is not changed by crystallization, as shown in Figure 3-3, parts a and b, the peak position does not change discontinuously but shifts somewhat to a smaller angular position with an increase in intensity. This suggests that the structure

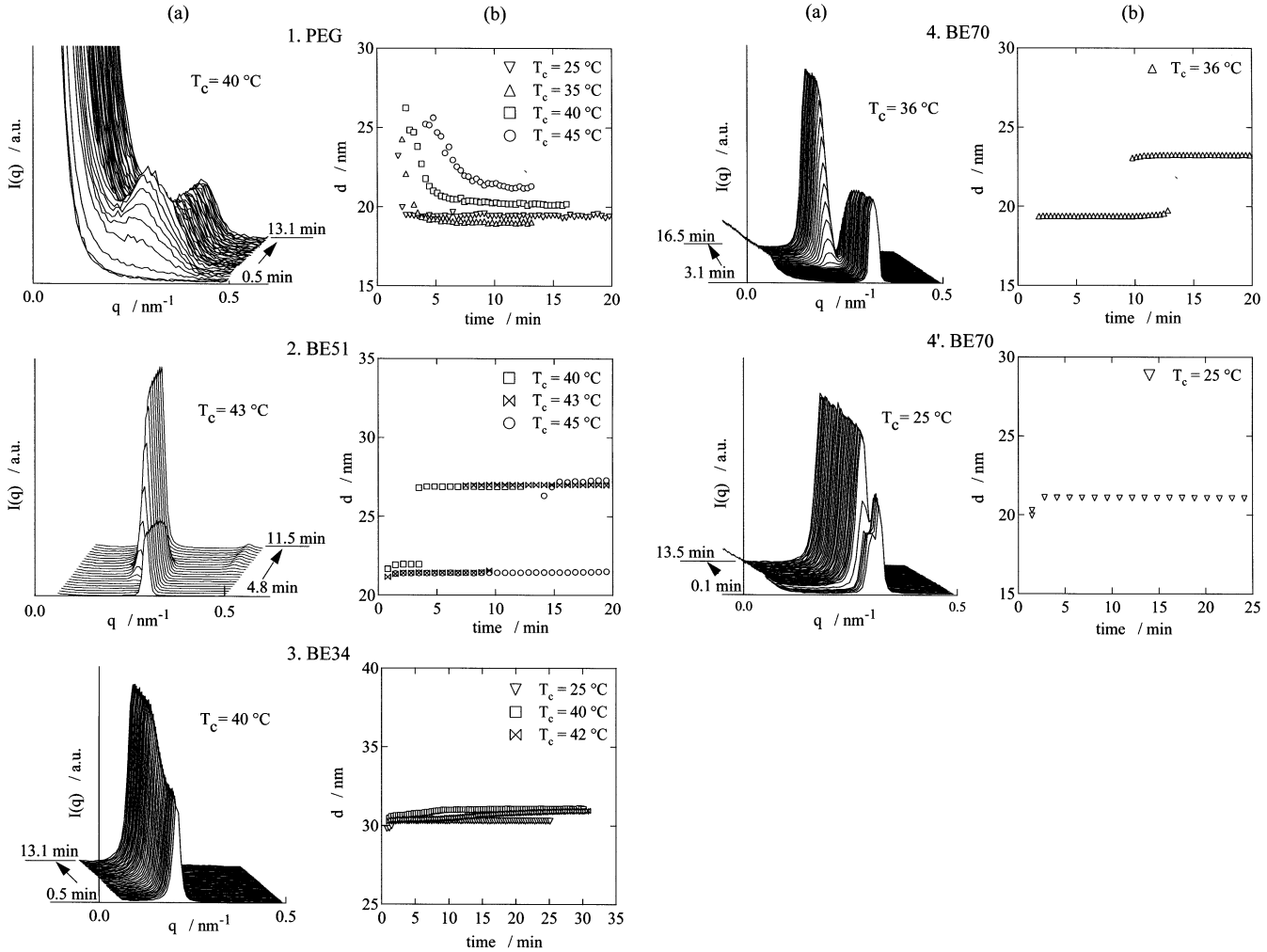

Figure 3. Time developments of (a) the first-order peak and (b) the Bragg spacing in the crystallization process of the homopolymer and diblock copolymers at the indicated crystallization temperatures.

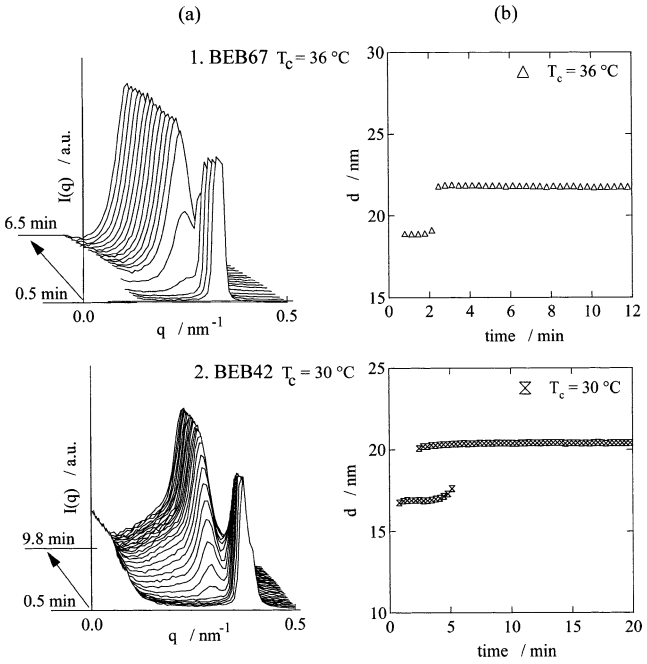

Figure 4. Behavior of (a) the first-order peak and (b) the Bragg spacing in the crystallization process of the triblock copolymers.

is not reorganized, that is, the PEG chains crystallize keeping the cylindrical microdomain in the melt. As shown in Figure 3, parts 4 and 4′, on the other hand, for BE70 the appearance of the peak due to the crystallization is accompanied by disappearance of that due to the microphase separation structure at both low and high crystallization temperatures; namely, the structure is reorganized by crystallization even though the morphology remains cylindrical.

As shown in Figure 4, the triblock copolymers, BEB67 and BEB42, have the same tendency in crystallization process as that of BE51, while the full width at half-maximum (fwhm) of the first-order peak in the crystalline state was larger for the triblock copolymers than for the diblock copolymers although their fwhm was almost the same among them in the melt. The wide fwhm may be due to polydispersity of the crystal lamella thickness. This polydispersity may be brought from disturbance of crystallization by the PBd chains bonded to both chain ends of PEG or from mixed conformations of loop- and bridge-types of the PEG chain in the lamellar structure of the melt.

The melting behavior for all the di- and triblock copolymers was the reverse of that in the crystallization process; the structure remained unchanged for BE34 while it was restructured for the other block copolymers.

In Figure 5 are summarized the Bragg spacings in the crystalline state plotted against the crystallization temperature together with those in the melt. The spacing of all the samples including the homopolymer increases nonlinearly with crystallization temperature. This corresponds to the theoretical prediction that the inverse of the lamella thickness is proportional to the melting temperature, i.e., crystallization temperature. A considerably large increase in BE70 may be attributed to the morphology change from cylinder to lamella at ca. 30 °C, because the Bragg spacing d in lattice plane (001) of lamellar structure is larger than that in the plane (100) of hexagonally packed cylindrical structure when the volume fraction is the same between their structures.

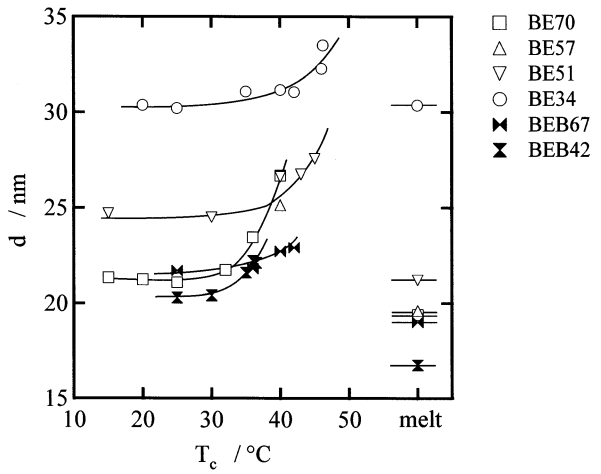

Figure 5. Dependence of the Bragg spacing on the crystallization temperature.

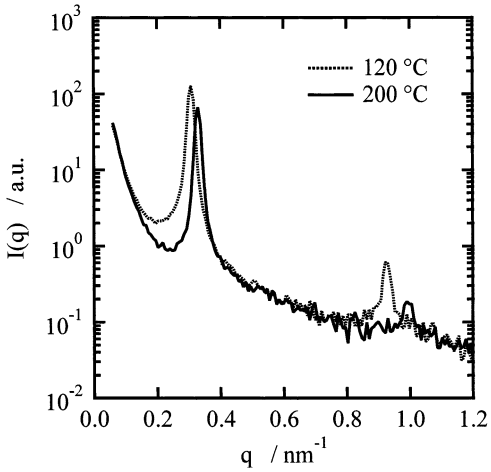

Figure 6. SAXS profiles of the PEG−PBd block copolymer with M_{PEG} = 7500 and M_{PBd} = 5500 at 120 and 200 °C.

(3) Discussion. As shown in Figure 6, clear SAXS peaks including higher-order peaks due to the microphase separation were observed for the PEG−PBd block copolymer even at 200 °C, which means that T_{ODT} is much higher than PEG's T_m. Although the Flory−Huggins χ parameter for PEG/PBd has not measured directly as far as we know,[12] this indicates that the degree of segregation of PEG−PBd copolymers is strong at crystallization temperatures studied here. Despite that, the experimental results obtained here suggest that the kinetic effects are also remarkable for structure formation or change on crystallization.

The typical example can be seen in crystallization from cylindrical melts for BE70. The PEG block of BE70 may be easily crystallized because it exists in the matrix, and the PBd chain can easily diffuse because the chain is short compared with PEG. Therefore, the structure change may be governed by competition between crystallization and diffusion rates. At high crystallization temperatures PEG crystallizes so slowly that the PBd chain can move enough to be rearranged, which can allow the block copolymers to form alternating lamellar structure of crystal lamella/amorphous layer, while at low temperatures the PBd chains may be left behind the crystallization of PEG because the crystallization rate is rapid. This behavior for BE70 can be attributed to kinetic aspects rather than the segregation degree.

Table 2. Apparent Equilibrium Melting Temperatures, Degrees of Crystallinity, and Avrami Indices in the Indicated Range of T_c

sample	T_c (°C)	$T_m°$ (°C)	DC (%)[a]	Avrami index
PEG5400	43.9−51.9	63.3	90.6−91.2	2.0−2.4
BE70	32.9−49.8	59.0	73.5−80.0	2.0−2.5
BE57	32.9−46.9	57.7	67.0−72.5	2.1−2.6
BE51	30.9−40.9	57.7	57.8−59.3	2.0−3.0
BE34	26.5−47.9	55.2	55.6−69.9	2.2−3.1
BEB67	37.8−49.8	57.7	58.0−69.3	2.0−3.0
BEB42	25.8−33.8	48.3	29.0−32.9	2.5−2.9

[a] Calculated using $\Delta H = 9.5$ kJ/mol for PEG.

In BE34 where the amorphous chains are in the matrix, on the other hand, it is difficult for the PBd chain to be rearranged accompanying crystallization. Quiram et al.[2,3] reported crystallization from cylinders. In the weakly segregated systems, crystallization of the fast cooled samples was confined to cylinders but slow crystallization destroyed the cylindrical melt structure to form alternating lamellar structure. In the strongly segregated one, why the position of the first-order SAXS peak did not shift so much though the higher-order peak position is not so clear. Chen et al.[13] examined the morphological change in crystallization for the blends of symmetrical PEG−PBd with a low molecular weight PBd homopolymer and observed that the melt morphology was not totally disrupted into lamellar morphology nor fully preserved in crystallization from both cylindrical and spherical domains. In their experiments, the samples were crystallized during cooling from +80 to −50 °C at −5 °C/min, which means that the crystallization temperature is over a wide range. Our sample BE34 was crystallized isothermally through rapidly quenching. These facts suggest that preservation of the cylindrical melt structure is caused by both kinetics and segregation factors.

BE51 exhibits the discontinuous structure change of lamellar to lamellar. Chen et al.[13] also showed that the scattering peaks of the PEG−PBd block copolymer with f(vol) = 0.50 and with almost the same molecular weight as BE51 shifted to a lower q position upon crystallization. Crystallization from lamellar melts is as easy as that of BE70 (as seen in crystallization rates later), and the rearrangement of the PBd chain can easily follow crystallization. These effects lead to reorganization of the structure in crystallization.

From the above consideration, it is concluded that the structure change in crystallization from microphase-separated melts depends on kinetic factors as well as the segregation degree and therefore on melt morphology.

3.2. Behavior of Crystallization from Microphase-Separated Melt. (1) Crystallinity and Melting Temperature. Degrees of crystallinity, DC, normalized to PEG content at various crystallization temperatures are summarized in Table 2. The crystallinity tends to decrease with a decrease in the copolymer composition of PEG. However, the degree of the decrease is not so much even in BE34, compared with that found for PTHF−PS block copolymers[10] in which T_m of PTHF is below T_g of PS. The crystallinities of PTHF−PS with f = 0.49 and 0.36 were 8.4 and 3.8%, respectively, and no crystallization was observed for the f = 0.27 copolymer. On the other hand, Nojima et al.[14] found that PCL−PBd copolymer with f = 0.26 could crystallize within a domain surrounded by the PBd matrix fixed with cross-linking. PTHF−PS must crystallize within the frozen microdomain surrounded by glassy PS, while the melt structures of PEG−PBd and PCL−PBd are not rigid because of rubbery PBd. Such comparison between PTHF−PS and PEG(or PCL)−PBd suggests that the block copolymers containing a flexibly movable amorphous component such as PBd can crystallize enough even within the cylindrical domain as well as the lamellar domain.

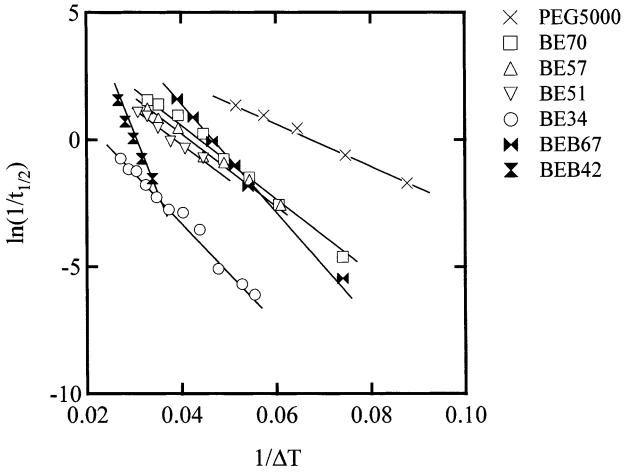

Figure 7. Arrhenius-type plots of the overall crystallization rate at $X_t = {}^1/_2$.

The crystallinity of the triblock copolymers, especially BEB42, is significantly smaller than that of the diblock copolymers with the nearly same composition, which means that crystallization of the middle chain in the triblock copolymers is suppressed by the amorphous block chains connected to both chain ends of the crystalline chain.

The apparent equilibrium melting temperatures $T_m°$ obtained by Hoffman−Weeks plots are also listed in Table 2. $T_m°$ of BEB42 is considerably low.

(2) Crystallization Kinetics. According to the Avrami equation, the fraction of crystallinity X_t at a crystallization time t is expressed as

$$X_t = 1 - \exp(-Kt^n) \tag{1}$$

where K is the overall crystallization rate and n is the Avrami exponent. Since eq 1 can be rewritten as

$$\log[-\ln(1 - X_t)] = \log K + n\log t \tag{2}$$

n can be evaluated from the initial slope of the plots of $\log[-\ln(1 - X_t)]$ vs $\log t$. As shown in Table 2, the values of n thus obtained are almost the same, i.e., 2−3, among all the block copolymers, whose values are not different from those of the homopolymer, even in BE34 which crystallizes within the cylindrical microdomain. This means that the dimensionality in crystallization growth for the present copolymers is not lowered. This is quite different from the case of PTHF−PS block copolymers[10] in which n is extremely small even for crystallization from the lamellar melt. This contrastive fact may be related to the difference between PTHF−PS and PEG−PBd described in section 3.2(1), that is, as described later, the values of n in PEG−PBd may reflect the fact that crystallization may propagate over a whole sample because of the flexible PBd chains.

The inverse of $t_{1/2}$ corresponds to the overall crystallization rate. Figure 7 shows plots of logarithm of $1/t_{1/2}$

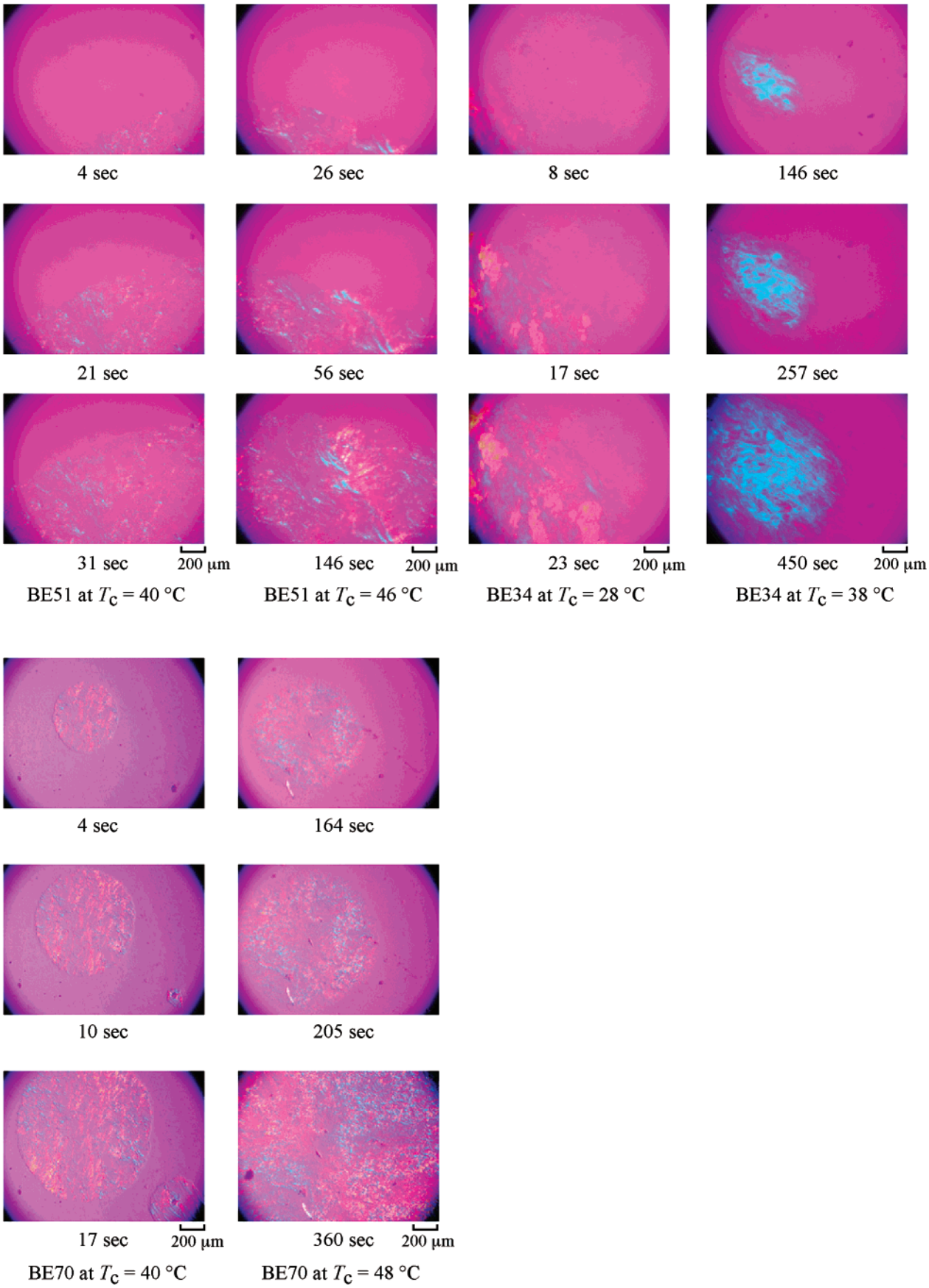

Figure 8. Propagation of the crystalline region observed by POM with a 530 nm retardation plate for the diblock copolymers at the indicated crystallization temperatures.

vs the inverse of the supercooling degree ΔT. The slope of the plots is almost the same among the diblock copolymers except for BE34. This means that the apparent activation energy of crystallization is almost

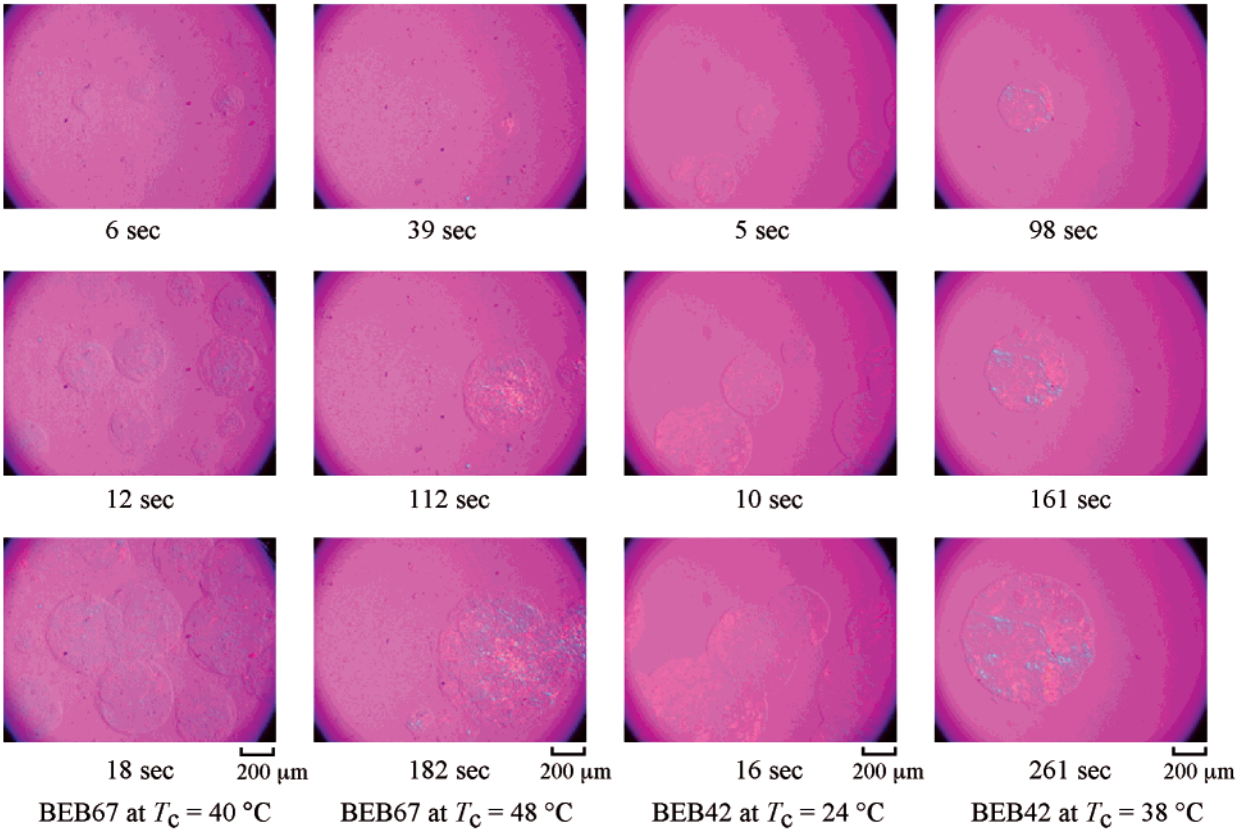

Figure 9. Propagation of the crystalline region observed by POM with a 530 nm retardation plate for the triblock copolymers at the indicated crystallization temperatures.

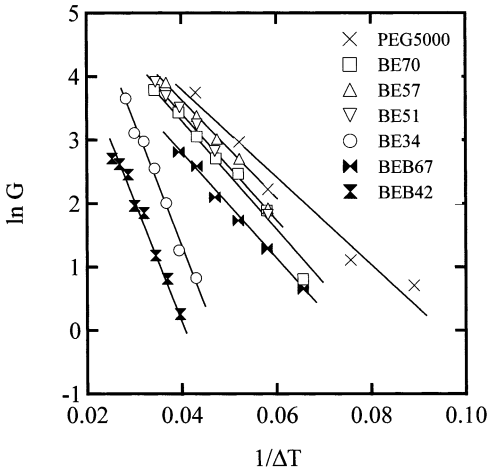

Figure 10. Arrhenius-type plots of the propagation rate observed by POM.

the same among the diblock copolymers whose structure is reorganized in crystallization. For BE34 which crystallizes keeping the melt microdomain, on the other hand, the apparent activation energy is somewhat higher and the crystallization rate is much slower.

The slope in the triblock copolymers is steeper than that of the diblock copolymers including BE34. This suggests that the crystallization kinetics are also affected by PBd connected to both chain ends of PEG in the same way as the degree of crystallinity. The crystallization rate for BEB42 is much slower than that for BEB67 despite their same lamellar morphology. This may be attributed to the size of the microdomain as well as the difference in the molecular weight of the PEG block. Furthermore, it should be noted that the overall crystallization rate at a large supercooling degree is rapider for the triblock copolymers than for the diblock copolymers. The overall rate at a large supercooling degree is attributed mainly to nucleation rates. It has been reported that the middle chain of ABA-type triblock copolymers takes a loop conformation of about 60%, which is more than a bridge conformation.[15−17] The former conformation may be more favorable to nucleation. This may be the reason for the rapider overall rate of the triblock copolymer at the large supercooling region.

Figures 8 and 9 show propagation of the crystalline region for the diblock and triblock copolymers, respectively, observed by polarizing optical microscopy (POM) with a retardation plate of 530 nm. No spherulite with a clear Maltese cross is observed for all the block copolymers studied here though four quadrants are dimly seen in BE70 at 48 °C, but blue- and yellow-colored crystalline regions are irregularly distributed. This shows that the crystal lamellae did not develop regularly like typical spherulites. Chen et al.[18] found the same behavior, and Hong et al.[19] also observed no spherulite. Here, it is noted that the crystal region propagates in an optical microscopic scale for BE34 as well as the other copolymers exhibiting reorganization. This shows that although the SAXS data suggest confinement of crystallization to the cylindrical domains, crystallization may traverse from one cylinder to another, which corresponds to the Avrami exponent of 2−3. Namely the crystallization is not confined completely to the cylindrical domain though the melt structure is not destroyed. This behavior of BE34 is different from that of PTHF−PS crystallized from frozen melts.

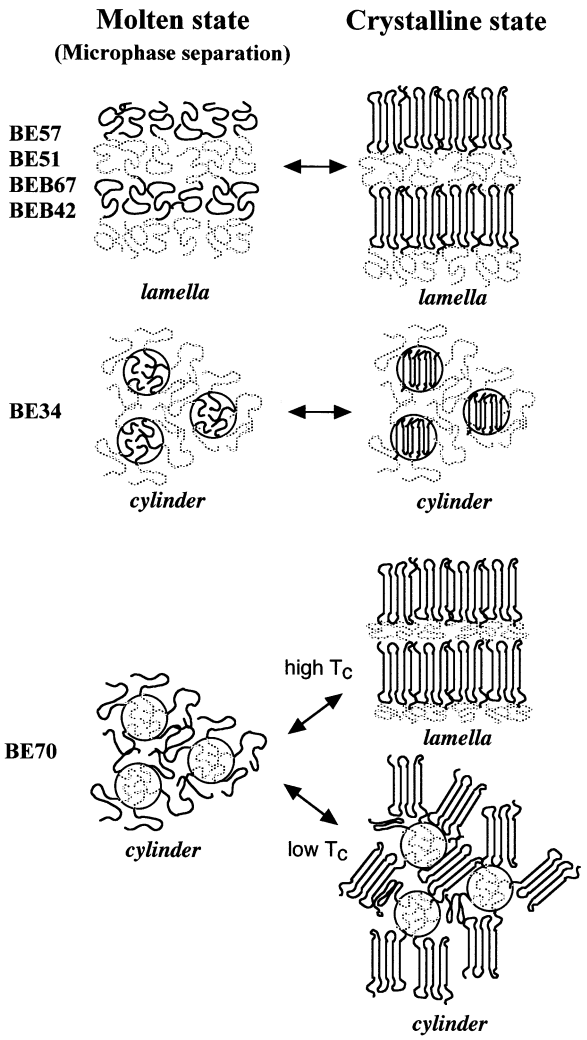

Figure 11. Schematic illustrations of the structure change between the molten and crystalline states of the block copolymers studied in the present work.

In the triblock copolymers, as shown in Figure 9, nucleation occurred in many places, especially at low crystallization temperatures. This supports the description about the overall crystallization rate: the middle chain in ABA block copolymers easily nucleates.

The propagation rates G of the crystalline region evaluated from the POM observation are shown in Figure 10, by Arrhenius-type plots against the inverse of the supercooling degree. The tendency of the plots for all the diblock copolymers is almost the same as that in the overall crystallization shown in Figure 7. However, it should be noted that the propagation (or growth) rate at low crystallization temperatures for the triblock copolymers is not rapider than that for the diblock copolymers, which is different from the behavior of the overall crystallization, because nucleation does not contribute to G so much. This comparison also suggests easy nucleation in the middle chain of the triblock copolymers.

4. Conclusion

Summarizing the results obtained from the SR−SAXS measurements, we can draw schematically the phase structure change between the molten and crystalline states as shown in Figure 11. In crystallization from the lamellar melt the structure is reorganized. The cylindrical structure containing a crystalline block in the matrix is maintained at low crystallization temperatures while it changes to lamellar structure at high crystallization temperatures. In the copolymers containing a crystalline block in the cylindrical domain, on the other hand, it crystallizes keeping the melt structure even though the crystallization is propagated beyond the microdomain. For the block copolymers with T_g (of amorphous chains) < T_m, considering both these observations and the previous results obtained by other investigators, it seems that morphology changes on crystallization from microphase-separated melts are governed by kinetic factors, i.e., competition between the crystallization and chain diffusion rates, as well as the degree of segregation. Therefore, whether melt structure is disrupted or not by crystallization depends on the supercooling degree, quenching rate, and melt morphology even in strongly segregated systems.

Even in the crystallization within the cylindrical domain, the Avrami exponent related to the dimension of the crystal growth is not small in PEG−PBd because crystals can traverse from a cylinder to another. This is quite different from crystallization from the frozen microphase-separated melt. On the other hand, both the rates of overall crystallization and crystal growth are considerably suppressed and the apparent activation energy is somewhat high in the crystallization from cylindrical domains.

The middle block in the triblock copolymer is easy to nucleate, but as a whole, the crystallization is disturbed by the amorphous chains.

Acknowledgment. This work was performed under the approval of the Photon Factory Program Advisory Committee (No. 00G034). The authors thank Drs. S. Nojima (Tokyo Institute of Technology) and S. Tanimoto (Japan Advanced Institute of Science and Technology, Hokuriku) for their technical advice on the SR−SAXS measurement. This work was supported financially by Grant-in-Aid for Sscientific Research (No. 11450365) from Japan Society for the Promotion of Science, by Grant-in-Aid for Scientific Research on Priority Areas (No. 13031033) from the Ministry of Education, Culture, Sports, Science and Technology, and by the Mitsubishi Foundation.

References and Notes

(1) Hamley, I. W. *The Physics of Block Copolymers*; Oxford: New York, 1998; Chapter 5.
(2) Quiram, D. J.; Register, R. A.; Marchand, G. R. *Macromolecules* **1997**, *30*, 4551.
(3) Quiram, D. J.; Register, R. A.; Marchand, G. R.; Ryan, A. J. *Macromolecules* **1997**, *30*, 8338.
(4) Hamley, I. W.; Fairclough, J. P. A.; Terrill, N. J.; Ryan, A. J.; Lipic, P. M.; Bates, F. S.; Towns-Andrews, E. *Macromolecules* **1996**, *29*, 8835.
(5) Nojima, S.; Kato, K.; Yamamoto, S.; Ashida, T. *Macromolecules* **1992**, *25*, 2237.
(6) Ryan, A. J.; Hamley, I. W.; Bras, W.; Bates, F. S. *Macromolecules* **1995**, *28*, 3860.
(7) Liu, L.-Z.; Yeh, R.; Chu, B. *Macromolecules* **1996**, *29*, 5336.
(8) Rangarajan, P.; Register, R. A.; Fetters, L. J.; Bras, W.; Naylor, S.; Ryan, A. J. *Macromolecules* **1995**, *28*, 4932.
(9) Sakurai, K.; MacKnight, W. J.; Lohse, D. J.; Schuluz, D. N.; Sissano, J. A. *Macromolecules* **1994**, *27*, 4941.
(10) Shiomi, T.; Tsukada, H.; Takeshita, K.; Takenaka, K.; Tezuka, Y. *Polymer* **2001**, *42*, 4997.
(11) Ueki, T.; Hiiragi, Y.; Kataoka, M.; Inoko, Y.; Amemiya, Y.; Izumi, Y.; Tagawa, H.; Muroga, Y. *Biophys. Chem.* **1985**, *23*, 115.

(12) Hong et al.[19] reported without any source that the χN was about 70 at 80 °C for the PEO/PBd with $M_{PEO} = 5600$ and $M_{PBd} = 5000$.
(13) Chen, H.-L.; Wu, J.-C.; Lin, T.-L.; Lin, J. S. *Macromolecules* **2001**, *34*, 6936.
(14) Nojima, S.; Hashizume, K.; Rohadi, A.; Sasaki, S. *Polymer* **1997**, *38*, 2711.
(15) Lin, Y. G.; Zhou, R.; Chien, J. C.; Winter, H. H. *Macromolecules* **1988**, *21*, 2014.
(16) Watanabe, H. *Macromolecules* **1995**, *28*, 5006.
(17) Watanabe, H.; Sato, T.; Osaki, K.; Yao, M.-L.; Yamagishi, H. *Macromolecules* **1997**, *30*, 5877.
(18) Chen, H.-L.; Hsiao, S.-C.; Lin, T.-L.; Yamauchi, K.; Hasegawa, H.; Hashimoto, T. *Macromolecules* **2001**, *34*, 671.
(19) Hong, S.; Yang, L.; MacKnight, W. J.; Gido, S. P. *Macromolecules* **2001**, *34*, 7009.

MA0200118